PHYSICAL REVIEW B
CONDENSED MATTER

THIRD SERIES, VOLUME 40, NUMBER 9 15 SEPTEMBER 1989-II

Thermodynamic properties of fcc transition metals as calculated with the embedded-atom method

S. M. Foiles and J. B. Adams
Theoretical Division, Sandia National Laboratories, Livermore, California 94551
(Received 13 March 1989)

Solid and liquid Gibbs free energies of Cu, Ag, Au, Ni, Pd, and Pt have been calculated through the use of the embedded-atom method, and the results are in good agreement with experiment. The melting points of the materials are calculated from the intersection of the solid and liquid free-energy curves. The values of the melting point are in excellent agreement for the noble metals and in reasonable agreement for Ni, Pd, and Pt. The thermal expansions of the solids are computed and the results are in excellent agreement with experiment over the entire temperature range.

I. INTRODUCTION

The embedded-atom method[1] (EAM) has become a popular method for computing the energetics of metallic systems for use with various computer simulation techniques. The ability to perform molecular-dynamics (MD) and Monte Carlo (MC) simulations with this approach makes it appealing to use in determining the high-temperature properties of metals and defects in metals. However, the experimental information used to determine the empirical functions in the EAM is all for zero-temperature solids (see below). It is therefore not clear that this approach will produce reliable high-temperature properties. In particular, it is known that the closely related N-body potentials developed by Finnis and Sinclair[2] fail to correctly predict the thermal expansion of the bcc metals.[3] In earlier work, Foiles and Daw[4] showed that the EAM correctly describes the room-temperature thermal expansion of the fcc metals provided that the functions are fit to the zero-temperature equation of state of the solid.

The primary purpose of this paper is to compute the thermodynamic properties of the solid and liquid phases of the fcc metals Cu, Ag, Au, Ni, Pd, and Pt as predicted by the EAM functions developed by Foiles, Baskes, and Daw (EAM-FBD).[5] This provides a stringent test of the interatomic interactions in this model. In particular, the Gibbs free energy of the solid and liquid phases are computed and compared with experiment. The melting points are determined from the intersections of the solid and liquid free energies. In addition, the thermal expansion of the solids is computed up to the melting point and compared with experiment. The calculations are performed by Monte Carlo simulations for both the solid and liquid phase and quasiharmonic (QH) approximation calculations for the solid phase.

In addition to providing a test of the EAM energetics, these results are potentially useful. The accurate knowledge of the melting point of this model is useful for studies of melting, solidification, or the properties of solid-liquid interfaces. For example, some of the early computer simulation work on the possibility of grain boundary premelting[6] was misinterpreted due to incorrect estimates of the bulk melting temperature.[7] Finally, if the EAM is found to provide an accurate description at high temperatures, the approach in this paper can be used to determine the thermodynamics of metastable amorphous and liquid phases and the high-temperature thermodynamics of point defects.

The next section will briefly review the EAM. This will be followed by a description of the calculational procedures for computing the free energies and equilibrium volumes of the solid and liquid phases. Finally, the results of the calculations will be compared to experiment for the fcc elements Cu, Ag, Au, Ni, Pd, and Pt.

II. EMBEDDED-ATOM METHOD

The embedded-atom method (EAM) is a semiempirical technique for computing the energy of an arbitrary arrangement of atoms. This approach has been widely used recently to study a variety of problems including point defect properties,[5] surface relaxations[5,8] and reconstructions,[9,10] surface and bulk phonons,[11,12] liquid structure,[13] thermal expansion,[4,14] segregation in alloys,[15] grain boundary structure,[16] and mechanical properties.[17] In this approximation, the energy is modeled as having two contributions: the energy to embed an atom into the local electron density provided by the remainder of the atoms and an electrostatic interaction represented by pair

interactions. In particular, the energy is written

$$E_{\rm tot}=\sum_i F_i(\rho_i)+\tfrac{1}{2}\sum_{i,j,i\neq j}\varphi_{ij}(R_{ij}) \ . \tag{1}$$

In this expression, ρ_i is the electron density at site i, F_i is the energy to place atom i into that electron density, and φ_{ij} is the pair interaction between atoms i and j. The electron density at each site is computed from a superposition of atomic electron densities,

$$\rho_i=\sum_{j\neq i}\rho_j^a(R_{ij}) \ , \tag{2}$$

where $\rho_j^a(R)$ is the atomic electron density of atom j at a distance R from its nucleus.

The embedding functions F and the pair interactions φ are determined empirically by adjusting them so that Eqs. (1) and (2) reproduce the zero-temperature equation of state of the solid, the elastic constants of the solid, and the vacancy formation energies. The requirement that the equation of state is reproduced is important since it introduces some information about the anharmonicity of the interactions into the potentials. The functions studied here were determined earlier by Foiles, Baskes, and Daw.[5] The EAM has the advantage that it includes certain many-body contributions to the energy though the computational effort is comparable to that required by pair interaction models. There are various other approaches which are similar to the EAM. The local volume potentials of Chen, Voter, and Srolovitz[18] and the glue model of Ercolessi, Tosatti, and Parinello[10] are essentially the same. The N-body potentials of Finnis and Sinclair[2] are also similar in practical application though the physical motivation behind the method is different. Derivations of the EAM energy form from first principles have been given by Jacobsen, Nørskov, and Puska[19] and by Daw.[20]

III. CALCULATION OF THE THERMODYNAMIC PROPERTIES

In this paper, we wish to compute the thermodynamic properties of the metals as described by the EAM. In particular, we are interested in the free energy, enthalpy, and equilibrium volume. The most reliable method of obtaining thermodynamic information is from either Monte Carlo or molecular-dynamics computer simulations. However, there are limitations to these methods. First, these simulation methods are classical. This is not a problem for temperatures greater than or on the order of the Debye temperature of the solid. (The Debye temperatures of the elements being studied here vary from around 170 K for Au to 375 K for Ni.[21]) However, below this temperature quantum mechanics significantly alters the thermodynamics through the freezing out of vibrational modes and zero-point contributions. Fortunately, for low temperatures, quasiharmonic methods (see below) provide a good quantum-mechanical description of the thermodynamics.

The other problem with the computer simulations for the determination of the thermodynamics is that the usual methods do not directly yield information about the entropy and so one cannot obtain the free energy. Free-energy differences between states at different temperatures within a given phase can be computed either by thermodynamic integration, as will be done here, or by using energy sampling techniques.[22] In the solid phase, the absolute free energy can be obtained at low temperatures from quasiharmonic calculations, as will be done here, or by a method due to Frenkel and Ladd.[23] In this approach, the free-energy difference between the actual solid and a reference Einstein model solid is computed. For the liquid phase, the calculation of the free energy is more difficult. The approach used here is to use MC simulations in the grand canonical ensemble.[24] Another method, due to Widom,[24,25] samples the energy associated with adding a test particle to the system at random locations. Finally, the free energy can be related to that of the ideal gas by a two-step process. First, the free-energy difference between the liquid and a reference liquid with purely repulsive interactions is computed. Then this latter system is expanded to a dilute gas and the change in free energy computed by thermodynamic integration. This latter method has been used recently by Broughton and Li[26] to compute the free energy of liquid Si.

The approach used here to obtain the free energies of the solid and liquid phases involves two steps. First, the free energy is obtained at some temperature in each phase. For the solid, quasiharmonic calculations at a temperature above the Debye temperature but below the point where anharmonic effects are important are used to obtain this value. (We will see below that such a range of temperatures does exist.) For the liquid, simulations in the grand canonical ensemble are performed at temperatures well above the melting point but below the boiling point. These yield the chemical potential and so the free energy at a point in the liquid phase as discussed below. The second step is to compute the enthalpy, which can be readily obtained from a MC simulation, for the desired range of temperatures. The Gibbs free energy at an arbitrary temperature can then be obtained by integrating over temperature using the expression

$$\frac{d}{dT}\left[\frac{G}{T}\right]_{N,P}=-\frac{H}{T^2} \ . \tag{3}$$

A. Quasiharmonic calculations

In the quasiharmonic approximation,[27] the full interatomic interactions are replaced by a quadratic expansion of the potential energy about the ideal lattice for each lattice constant, a. Anharmonic effects are included only through the variation of the quadratic expansion with lattice constant and through the variation of the ideal lattice energy with the lattice constant. At each lattice constant, the system is equivalent to a collection of harmonic oscillators. The Helmholtz free energy F of a solid with lattice constant a and temperature T is

$$F(a,T)=E_0(a)+k_BT\sum_{\mathbf{k},j}\ln 2\left[\sinh\frac{\hbar\omega_j(\mathbf{k})}{2k_BT}\right] \ . \tag{4}$$

In this expression, $E_0(a)$ is the energy of the ideal static

lattice evaluated for the lattice constant a, the sum is over the different phonon polarizations, j, and wave vectors $\mathbf{k}$ in the Brillouin zone, and $\omega_j(\mathbf{k})$ is the frequency of the phonon modes. There is an implicit dependence of the frequencies $\omega_j(\mathbf{k})$ on the lattice constant. The procedure for computing the phonon frequencies within the EAM is described by Daw and Hatcher.[11] Equation (4) yields the free energy as a function of lattice constant, or equivalently volume, and temperature. The free energy and volume at zero pressure is then obtained by minimizing this expression with respect to the lattice constant for each temperature. Other thermodynamic properties, such as the entropy and enthalpy, can be computed by similar sums over the phonon modes.[27] This approach has been used earlier to compute the room-temperature coefficient of thermal expansion for the EAM-FBD.[4]

B. Monte Carlo simulations

The general technique of using Monte Carlo simulations in statistical mechanics has been extensively discussed and reviewed in the literature. In the following, the general method will be outlined. For a discussion of the theoretical basis of the approach and other applications see, for example, the books edited by Binder.[24] The goal of the simulations is to produce a series of atomic configurations such that the probability of a configuration being generated in this series is proportional to the probability of the configuration occurring in the statistical ensemble. This is achieved by numerous repetitions of the following cycle. Start with some atomic configuration denoted by i with statistical probability P_i. The arrangement of the atoms is then changed to produce a new configuration, j, and the relative statistical probabilities of the two configurations, P_j/P_i, is computed (see below). If this ratio is greater than unity, the new configuration j is retained. If the ratio is less than unity, the new configuration is retained with a probability given by the ratio P_j/P_i. If the new configuration is not retained, the system returns to configuration i. This process is repeated numerous times (10^4–10^5 per atom). The result is that configurations are generated by this process with the probability P_i. Thus to compute the equilibrium properties of the system, one simply averages the desired quantity over the configurations that are generated. The two quantities of interest here are the internal energy and the pressure. The internal energy is evaluated using Eqs. (1) and (2). The pressure can be evaluated in the EAM using the virial expression

$$PV = Nk_BT - \frac{1}{3}\left[\sum_{i,j,i\neq j}[F_i'(\rho_i)\rho_j^{a'}(R_{ij}) + \tfrac{1}{2}\varphi'(R_{ij})]R_{ij}\right] . \tag{5}$$

This procedure requires that one can compute the relative probabilities of two configurations, i.e., P_j/P_i. For the case of the canonical ensemble where the number of atoms, the volume, and the temperature are held constant, the probability of configuration i is just the Boltzmann distribution

$$P_i = \frac{1}{Z}e^{-E_i/k_BT} . \tag{6}$$

In this expression, E_i is the energy of configuration i, Z is the partition function, and T is the temperature. In this case the ratio of the probabilities just reduces to the Boltzmann factor associated with the energy difference between the two configurations, i.e.,

$$\frac{P_j}{P_i} = e^{-(E_j-E_i)/k_BT} . \tag{7}$$

In the canonical ensemble, therefore, determining the relative probability of two configurations reduces to computing the energy difference between them.

In practice, it is often desirable to fix the pressure of the system rather than the volume. The simulation can then be performed in the isothermal-isobaric ensemble. In this ensemble, the relative statistical probabilities of two configurations i and j are

$$\frac{P_j}{P_i} = \left[\frac{V_j}{V_i}\right]^N \exp\{-[E_j-E_i+P(V_j-V_i)]/k_BT\} . \tag{8}$$

In this expression, V_i is the volume of the system for configuration i and P is the desired pressure of the system. The changes in the volume are accomplished by an expansion or contraction of the periodically repeated cell. In the present calculations, the cell is also allowed to distort orthorhombically.

To obtain the free energy in the liquid phase, Monte Carlo simulations in the grand canonical ensemble can be used. In this ensemble, the temperature, volume, and chemical potential of the system are held fixed and atoms can be created or destroyed during the simulation. From such a simulation, one can calculate the energy, pressure, and density for the given temperature and chemical potential. Since the chemical potential of the one-component system is just $\mu = G/N$, the Gibbs free energy per atom, such a simulation relates the free energy to the temperature and pressure. The probability of a given configuration in this ensemble is proportional to

$$P_i \propto \frac{1}{N_i!}\left[\frac{V}{\Lambda^3}\right]^{N_i} \exp[-(E_i - N_i\mu)/k_BT] . \tag{9}$$

In this expression, N_i is the number of atoms, E_i is the potential energy of the configuration, V is the volume, and Λ is the thermal de Broglie wavelength of the atom. The simulations include two types of changes to the system. The first is small displacements of the atoms. For such changes, the only term that remains in the ratio of the probabilities is the Boltzmann factor as in the case of the canonical ensemble. The other change to the system is to create or destroy an atom. In the case of creating an atom, the position of the atom is chosen at random in the simulation cell. The computational bottleneck is that Monte Carlo steps which create and destroy atoms are seldom accepted. This means that a very long simulation is required to produce statistically significant results. This problem is less severe at higher temperatures and

lower densities. That is why the simulations here were performed at temperatures of about twice the melting point.

In a grand canonical simulation, one chooses the chemical potential, temperature, and volume. In the current case, what we want is the chemical potential at zero pressure. One can obtain this by a trial and error series of simulations at various chemical potentials and from these results determine the chemical potential that yields zero pressure. This process is aided by the Maxwell relation

$$\left[\frac{\partial P}{\partial \mu}\right]_{V,T} = \left[\frac{\partial N}{\partial V}\right]_{\mu,T} = \frac{N}{V} \tag{10}$$

which relates the derivative of the pressure with respect to the chemical potential to computable quantities. In practice, an estimate of the chemical potential at zero pressure is determined. Then several simulations are performed at chemical potentials near this value (within $\sim 0.2 k_B T$). The pressure as a function of chemical potential is then assumed to have a quadratic behavior with the coefficients determined by a simultaneous least-squares fit to the pressure and to the derivative of the pressure with respect to chemical potential at each chemical potential simulated. The chemical potential at zero pressure is then determined from this quadratic fit.

IV. RESULTS AND DISCUSSION

A. Gibbs free energy

The Gibbs-free-energy curves for the solid and liquid phases computed as described above are compared with experiment[28] in Fig. 1. The Gibbs free energy is referenced to that of the solid fcc phase at 300 K. In general, the agreement between experiment and theory is quite good for both the solid and liquid phases. It is surprising that the EAM describes the Gibbs free energy of the solid phase at elevated temperatures, since it is only fit to properties of the bulk solid at 0 K or room temperature. It is especially surprising that the EAM describes the *liquid* phase, since the EAM functions were fit only to parameters of the *bulk solid* phase.

The EAM functions for Ag, Cu, and Pd are in especially good agreement with experiment in predicting the Gibbs free energies of the solid phase. The functions for Au and Pt are in slightly less agreement, and the Ni function is in the least agreement. The same trends generally hold true for predictions of the free energy of the liquid phase, except that the Pd functions are slightly worse in predicting the liquid phase. For Au, Pd, and Pt, the predicted free energies of both solid and liquid phases are always slightly *lower* than experimental values, whereas for Ni the predictions are *higher* than experiment.

Recall that the calculation of the Gibbs free energy at moderate to high temperatures uses the enthalpy from the MC calculations with Eq. (3) to extend the QH values of the free energy to higher temperatures. This approximation required that there exists a temperature range for which both methods yield the same results. Figure 2 shows a comparison of the Gibbs free energy of solid Ni,

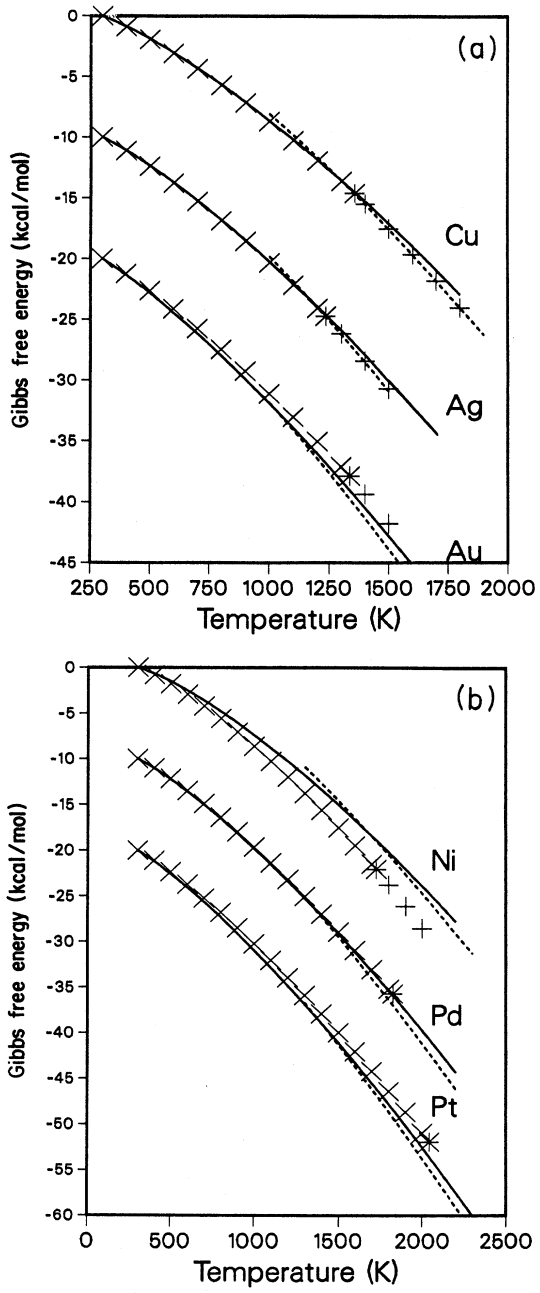

FIG. 1. Gibbs free energy of the solid and liquid phases of (a) Cu, Ag, and Au and (b) Ni, Pd, and Pt in units of kcal/mole and referenced to the free energy at 300 K. The vertical axis applies to the results for Ni and Cu with the other curves offset by 10 kcal/mole. The points represent the experimental values ($\times$ for solid and $+$ for liquid phase) from Ref. 28. The solid curves are the EAM solid free energies and the dashed curves are the EAM liquid free energies.

as calculated by the QH techniques and by integrating the MC enthalpies. They show excellent agreement up to the melting point, and the agreement is equally good for all the other metals (better than 2% accuracy at the melting point). This level of agreement is interesting since the QH technique approximates the anharmonic contribu-

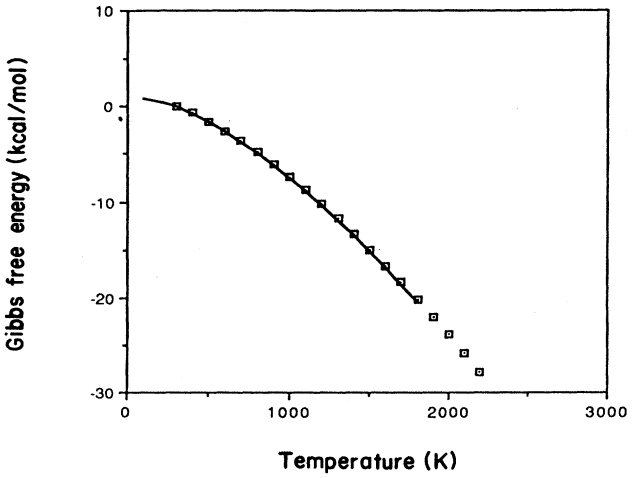

FIG. 2. Comparison of QH (squares) and MC (solid lines) calculations of Gibbs free energy of solid Ni in units of kcal/mole.

tions to the energy. This is an important result since MC calculations of the thermodynamic properties require a couple of orders of magnitude more computer effort than the QH calculations.

B. Melting point

The melting point may be determined by the intersection of the Gibbs free energy curves of the liquid and solid phases (see Fig. 1). Table I summarizes the melting-point information for the elements. In all cases except Ni, the calculated values are lower than the experimental values. The agreement is quite good for Ag, Cu, and Ni, somewhat poorer for Au, and off by almost 600 K for Pd and Pt. The good agreement for Ag and Cu is consistent with the accurate prediction of the Gibbs free energies. The good agreement for Ni is totally fortuitous, since both the solid and liquid free-energy curves are too high, but the errors offset one another. The discrepancies for Au and Pt are somewhat to be expected, since their free-energy curves are somewhat inaccurate. The discrepancy for Pd is quite interesting: the free energy of the solid phase is accurately predicted, but the prediction for the liquid phase is low.

It is important to realize that small inaccuracies in the free-energy curves may lead to large errors in predictions of the melting point. The difference in the slopes of the solid and liquid free energies is given by $\Delta H/T_m$, where

TABLE I. Comparison of theoretical and experimental melting points (in K).

Element	mp (MC)	mp (Expt)
Ag	1170	1234
Au	1090	1338
Cu	1340	1358
Ni	1740	1726
Pd	1390	1825
Pt	1480	2045

ΔH is the latent heat of melting and T_m is the melting point. This ranges for the elements considered here from 0.93 to 1.03×10^{-4} eV/(atom K) for Ag and Ni, respectively.[29] Thus an error of 0.01 eV in the Gibbs free energy per atom can lead to an error of 100 K in the melting point. (The simulations were performed until the statistical uncertainty in the energies was less than 0.002 eV.) Also, as in some cases of Ni, it is possible to get a good value of the melting point even though the free energies are in error. Consequently, it is far more informative to calculate Gibbs free energies than to simply calculate melting points.

As a comparison, the melting point was also estimated for Ni by a MD simulation technique. The basic idea is to determine the temperature at which a sample melts. There are two problems with this approach. First of all, unless the solid already contains a free surface, there is a nucleation barrier to melting due to the liquid-solid interface energy. Secondly, computer simulations are limited to very short times, on the order of picoseconds, so the solid may not melt during the simulation even if it is above the melting point. Therefore, this simple method tends to overestimate the melting point of the potential.

However, both of the above limitations may be overcome by beginning with a material containing both a liquid and a solid. The liquid and solid should be geometrically arranged such that the solid-liquid interface remains constant in area as freezing or melting occurs. For example, imagine a cube of liquid in contact with a cube of solid. This configuration removes the nucleation barrier due to interface energy. MD runs for several picoseconds are typically long enough for the interface to move provided that the temperature is not near the melting point. If either the solid or liquid phase grows, then the temperature of the simulation is known to be above or below the melting point. It is important in these calculations that the MD simulations are performed at constant temperature rather than at constant energy. If the simulation is at constant energy, then the motion of the interface is suppressed since there is no source or sink for the energy associated with the latent heat of the materials that transforms between phases.

The above MD technique was used to calculate the melting point of the EAM-FBD function for Ni. The starting configuration was a rectangular solid in contact with a rectangular liquid region. The material was then held at constant temperature (1400–2000 K) for up to 10 picoseconds. For temperatures from 1400 to 1600 K, the interface region slowly advanced into the liquid region, solidifying the liquid. For temperatures from 1800 to 2000 K, the reverse occurred. For temperatures of 1600 to 1800 K, the interface did not move significantly, since the driving force for solidification and/or melting (the difference in Gibbs free energies between the liquid and solid) was small. Thus, the melting point was found to be between 1600 and 1800 K which is consistent with the value of 1740 K determined from the free energies. The melting point can be determined even more accurately by extrapolating the rate of motion of the solid-liquid interface to zero velocity, since the velocity increases as the difference between the temperature and the melting point

is increased.[30]

C. Thermal expansion

Both QH and MC techniques were also used to calculate the lattice constant of the solid phase over the entire temperature range. (In previous work, Foiles and Daw[4] computed the coefficient of thermal expansion at room temperature using the QH approximation.) The QH approximation is expected to be more accurate at low temperatures since it includes quantum effects (zero-point motion and freezing out of modes) which are ignored in the classical MC simulations. The MC results should be more reliable at high temperature since it fully includes anharmonic effects. Figure 3 compares the QH and MC results for Ag. The values of the expansion are normalized by the QH values for the lattice constant at 0 K. At low temperatures the MC computed lattice constant is smaller than the QH value due to the neglect of zero-point motion in the MC calculations. At moderate temperatures, the two approaches agree well. The difference between the QH and MC results at high temperature was largest for the case of Ag, smaller for Ni and Pt, and smallest for Cu, Au, and Pd.

Figure 4 compares the calculated thermal expansion with the experimental values for the six elements studied. The calculated values are taken from the QH calculations below 500 K and from the MC calculations above 500 K. In general, the shape of the calculated thermal expansion curves are in excellent qualitative agreement with experiment.[31] The thermal expansion of Cu and Ni are the best (the two highest experimental data points for Ni are suspected of being inaccurate[31]). The calculated thermal expansion of Au and Pd were almost as accurate, and predictions for Ag and Pt were the worst, although still reasonable. The predicted values for Ag, Au, and Ni were too high, and the predicted values for Pd and Pt were too low.

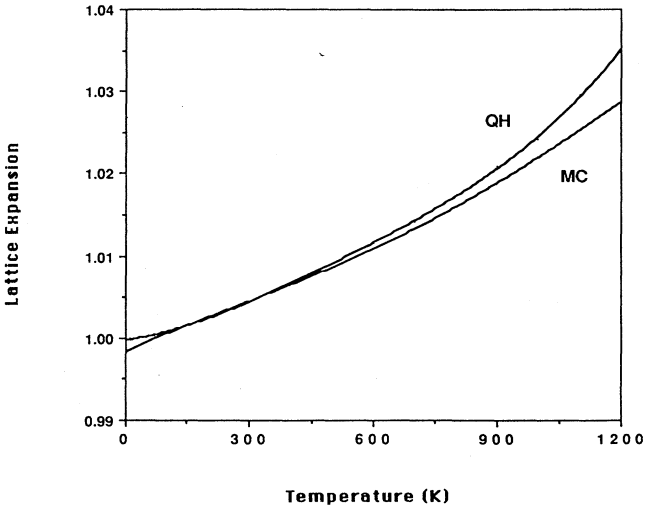

FIG. 3. Comparison of QH and MC calculations of thermal expansion of solid Ni. The difference between the two curves is due primarily to the neglect of zero-point motion in the MC simulations.

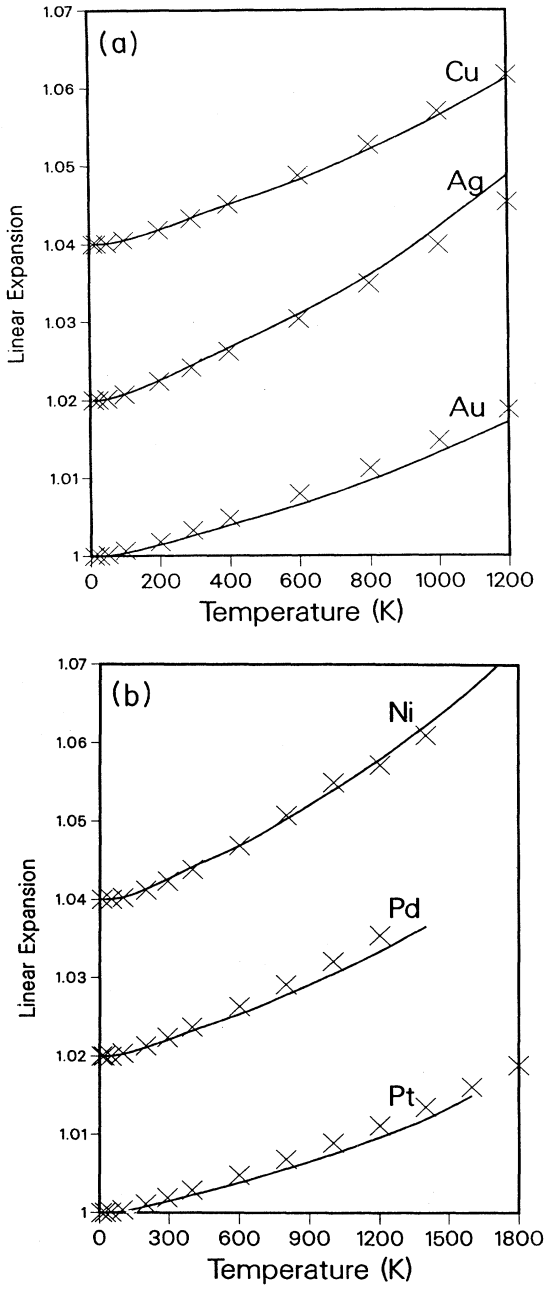

FIG. 4. Linear thermal expansion of (a) Cu, Ag, and Au and (b) Ni, Pd, and Pt. The vertical axis applies to Au and Pt and the other curves are offset by 0.02. The experimental data from Ref. 31 are plotted as points, and the calculated values are plotted as curves. Note that the two highest temperature experimental points for Ni are suspect (Ref. 31).

The accurate prediction of both the thermal expansion and the free energy implies that the average Gruneisen constant of the system is correct. The Gruneisen constant γ is related to the average derivative of the phonon frequencies with respect to volume changes.[20] It is related to the linear coefficient of thermal expansion, α, by

$$\alpha=\frac{\gamma c_v}{3B}\ , \tag{11}$$

where c_v is the specific heat and B is the bulk modulus. Since the results for the free energy suggest that c_v is accurately described and the bulk modulus is also correctly predicted by this model, the Gruneisen parameter must be accurately reproduced. This implies that the variation of the phonon frequencies and so the interatomic force constants with volume is accurately reproduced.

V. SUMMARY

The QH and MC techniques were shown to be capable of determining the Gibbs free energy of solid phases, and the MC technique could also handle liquids. The two methods were shown to agree to within 2% for the solid phase even near the melting point, which is important since the QH calculations are much less computationally intensive. Also, both MD techniques and comparison of Gibbs free energies (from MC) were used to determine the melting points associated with the EAM-FBD energetics. The two methods agreed with one another for the case of Ni (the only case examined) and the computed melting points are in reasonable accord with the experimental values. Finally, QH and MC techniques were used to calculate thermal expansion of the metals.

The FBD functions yielded qualitatively correct values for the Gibbs free energy and thermal expansion, although some of the functions were more quantitatively accurate than others. Small inaccuracies in Gibbs free energies may lead to large inaccuracies in the melting points. It is especially encouraging that the EAM-FBD functions predict the properties of liquids fairly accurately, since they were fit only to the properties of bulk solids. This strongly suggests that the EAM correctly approximates much of the actual physics. Of the EAM-FBD functions, the Cu function was the most successful in predicting the Gibbs free energy of the solid and liquid, as well as the thermal expansion of the solid.

ACKNOWLEDGMENTS

The authors wish to acknowledge the work of Dr. Murray Daw of this laboratory in developing the computer codes for the quasiharmonic calculations and the technical assistance of Ms. Denise Vickers in performing the various calculations. This work supported by the U.S. Department of Energy, Office of Basic Energy Sciences, Division of Materials Sciences.

[1]M. S. Daw and M. I. Baskes, Phys. Rev. Lett. **50**, 1285 (1983); Phys. Rev. B **29**, 6443 (1984).
[2]M. W. Finnis and J. E. Sinclair, Philos. Mag. B **50**, 45 (1984).
[3]M. Marchese, G. Jacucci, and C. P. Flynn, Philos. Mag. Lett. **57**, 25 (1988).
[4]S. M. Foiles and M. S. Daw, Phys. Rev. B **38**, 12 643 (1988).
[5]S. M. Foiles, M. I. Baskes, and M. S. Daw, Phys. Rev. B **33**, 7983 (1986).
[6]T. Nguyen, P. S. Ho, T. Kwok, C. Nitta, and S. Yip, Phys. Rev. Lett. **57**, 1919 (1986).
[7]S. Yip, private communication.
[8]N. Ting, Y. Qingliang, and Y. E. Yiying, Surf. Sci. **206**, L857 (1988).
[9]M. S. Daw and S. M. Foiles, Phys. Rev. Lett. **59**, 2756 (1987); B. W. Dodson, Phys. Rev. B **35**, 880 (1987).
[10]F. Ercolessi, E. Tosatti, and M. Parinello, Phys. Rev. Lett. **57**, 719 (1986).
[11]M. S. Daw and R. D. Hatcher, Solid State Commun. **56**, 697 (1985). There is a typographical error in Eq. (4): F' should be replaced by $2F'$ in both places.
[12]J. S. Nelson, E. C. Sowa, and M. S. Daw, Phys. Rev. Lett. **61**, 1977 (1988); L. Ningsheng, X. Wenlan, and S. C. Shen, Solid State Commun. **67**, 837 (1988).
[13]S. M. Foiles, Phys. Rev. B **32**, 3409 (1985).
[14]P. Stoltze, K. W. Jacobsen, and J. K. Nørskov, Phys. Rev. B **36**, 5035 (1987).
[15]S. M. Foiles, Phys. Rev. B **32**, 7685 (1985); S. M. Foiles, in Surface Segregation and Related Phenomena, edited by P. A. Dowben and A. Miller (Chemical Rubber Co., Cleveland, in press).
[16]S. M. Foiles, Acta Metall. (to be published).
[17]M. S. Daw, M. I. Baskes, C. L. Bisson, and W. G. Wolfer, *Modeling Environmental Effects on Crack Growth Processes,* edited by R. H. Jones and W. W. Gerberich (Metallurgical Society of AIME, New York, 1986).
[18]S. P. Chen, A. F. Voter, and D. J. Srolovitz, Phys. Rev. Lett. **57**, 1308 (1986); S. P. Chen, D. J. Srolovitz, and A. F. Voter, J. Mater. Res. **4**, 62 (1989).
[19]K. W. Jacobsen, J. K. Nørskov, and M. J. Puska, Phys. Rev. B **35**, 7423 (1987).
[20]M. S. Daw, Phys. Rev. B **39**, 7441 (1989).
[21]N. W. Ashcroft and N. D. Mermin, *Solid State Physics* (Holt, Rinehart and Winston, New York, 1976).
[22]J. P. Valleau and G. M. Torrie, in *Modern Theoretical Chemistry,* edited by B. J. Berne (Plenum, New York, 1976), Vol. 5.
[23]D. Frenkel and A. J. C. Ladd, J. Chem. Phys. **81**, 3188 (1984).
[24]*Monte Carlo Methods in Statistical Physics,* 2nd ed. edited by K. Binder (Springer-Verlag, New York, 1986); *Applications of the Monte Carlo Method in Statistical Physics,* edited by K. Binder (Springer-Verlag, New York, 1984).
[25]B. Widom, J. Chem. Phys. **39**, 2808 (1963).
[26]J. Q. Broughton and X. P. Li, Phys. Rev. B **35**, 9120 (1987).
[27]A. A. Maradudin, E. W. Montroll, G. H. Weiss, and I. P. Ipatova, *Theory of Lattice Dynamics in the Harmonic Approximation* (Academic, New York, 1971), 2nd ed. (Suppl. 3 in the *Solid State Physics* series, edited by H. Ehrenreich, F. Seitz, and D. Turnbull).
[28]R. Hultgren, P. D. Desai, D. T. Hawkins, M. Gleiser, K. K. Kelly, and D. D. Wagman, *Selected Values of the Thermodynamic Properties of the Elements* (American Society for Metals, Metals Park, Ohio, 1973).
[29]*Smithells Metals Reference Book,* 6th ed., edited by E. A. Brandes (Butterworths, London, 1983).
[30]J. F. Lutzko, D. Wolf, S. Yip, S. R. Phillpot, and T. Nguyen, Phys. Rev. B **38**, 11 572 (1988).
[31]Y. S. Touloukian, R. K. Kirby, R. E. Taylor, and P. D. Desai, *Thermophysical Properties of Matter, Vol. 12: Thermal Expansion–Metallic Elements and Alloys* (Plenum, New York, 1975).